

# Enigmatic presence of mitochondrial complex I in Trypanosoma brucei bloodstream forms



EC
Journals.ASM.org

# Enigmatic Presence of Mitochondrial Complex I in *Trypanosoma brucei* Bloodstream Forms

**Sachin Surve,[a] Meredith Heestand,[a] Brian Panicucci,[a]* Achim Schnaufer,[a,b] and Marilyn Parsons[a,c]**

Seattle Biomedical Research Institute, Seattle, Washington, USA[a]; Institute of Immunology & Infection Research and Centre of Immunity, Infection & Evolution, The University of Edinburgh, Edinburgh, United Kingdom[b]; and Department of Global Health, University of Washington, Seattle, Washington, USA[c]

**The presence of mitochondrial respiratory complex I in the pathogenic bloodstream stages of *Trypanosoma brucei* has been vigorously debated: increased expression of mitochondrially encoded functional complex I mRNAs is countered by low levels of enzymatic activity that show marginal inhibition by the specific inhibitor rotenone. We now show that epitope-tagged versions of multiple complex I subunits assemble into $\alpha$ and $\beta$ subcomplexes in the bloodstream stage and that these subcomplexes require the mitochondrial genome for their assembly. Despite the presence of these large (740- and 855-kDa) multisubunit complexes, the electron transport activity of complex I is not essential under experimental conditions since null mutants of two core genes (*NUBM* and *NUKM*) showed no growth defect *in vitro* or in mouse infection. Furthermore, the null mutants showed no decrease in NADH:ubiquinone oxidoreductase activity, suggesting that the observed activity is not contributed by complex I. This work conclusively shows that despite the synthesis and assembly of subunit proteins, the enzymatic function of the largest respiratory complex is neither significant nor important in the bloodstream stage. This situation appears to be in striking contrast to that for the other respiratory complexes in this parasite, where physical presence in a life-cycle stage always indicates functional significance.**

*Trypanosoma brucei* subspecies are single-celled protozoan parasites that cause human African trypanosomiasis, or sleeping sickness, and a variety of related diseases in animals. Their life cycles include development in the tsetse fly vector and a mammalian host. Within the mammalian host, *T. brucei* bloodstream forms (BFs) proliferate as slender forms, some of which develop into nonproliferating stumpy forms that show specific metabolic adaptations presaging the next developmental stage within the fly midgut (procyclic forms [PFs]). Among the differences between BFs and PFs are major alterations in mitochondrial metabolism (62). For instance, PFs derive their energy mostly by proline metabolism, which employs mitochondrial enzymes (14), while BFs rely exclusively on glucose and glycolysis for their energy needs (39). In many eukaryotes, the glycolytic pathway is followed by the mitochondrial Krebs cycle, which is linked to the respiratory electron transport chain to allow the generation of many additional ATP molecules. However, in trypanosomes as well as many other protozoa, the situation is more complex and the Krebs cycle enzymes, although present, are not linked in a complete cycle. Respiratory complexes III and IV are present and functional in PFs but absent in BFs. In contrast, complex V is present in both stages (5, 6, 60). While there are reports of the first enzyme complex (complex I [cI]) in the respiratory chain in PFs (1, 21, 43, 61), its presence and functionality in BFs have been debated (40).

Complex I (NADH:ubiquinone oxidoreductase [EC 1.6.5.3]) resides in the plasma membrane of prokaryotes and mitochondrial inner membrane of eukaryotes, where it catalyzes the oxidation of NADH and transfers electrons to coenzyme Q (23, 41). The energy thus acquired is used to pump protons across the membrane. Crystallographic studies of prokaryotic cI have shown that the hydrophilic arm functioning in electron transfer extends into the cytosol at a right angle to the hydrophobic, proton-pumping arm embedded in the membrane (18, 27). Prokaryotic cI is composed of 14 subunits; these subunits make up the core complex (23). Mammalian cI additionally contains up to 32 accessory subunits (11), some of which are involved in assembly of the complex (50).

Bioinformatic analyses of the *T. brucei* nuclear and mitochondrial genomes identified 19 conserved subunits of cI, but 2 core subunits were not found: NULM (ND4L) and NU6M (ND6) (29, 40, 56, 57). These subunits reside in the hydrophobic membrane arm and are thought to be essential for proton pumping (68). Thus, it has been suggested that in *T. brucei* cI does not participate in forming the electrochemical gradient of the mitochondrion (40). The underlying assumption for this proposal is questioned by recent data from the yeast *Yarrowia lipolytica* that suggest that proton pumping may occur via two distinct modules (proximal and distal) (17). This raises the possibility that *T. brucei* cI could still function in that process. Adding to the controversy on the presence of functional cI in *T. brucei* (40) are the high concentrations of the cI inhibitor rotenone required for inhibition (raising questions of off-target activity) and the presence of the alternative NADH dehydrogenase NDH2 (20), which could confound enzymatic assays. Nonetheless, cumulative evidence now indicates the presence of cI in PFs. First, in addition to NADH dehydrogenase activity that is moderately sensitive to rotenone, immunodetection of cI subunits was reported (21). Second, proteomic analysis

**Received** 1 November 2011 **Accepted** 28 November 2011
**Published ahead of print** 9 December 2011
Address correspondence to Achim Schnaufer, achim.schnaufer@ed.ac.uk, or Marilyn Parsons, marilyn.parsons@seattlebiomed.org.
* Present address: Biology Center, Institute of Parasitology, Ceske Budejovice, Czech Republic.
A. Schnaufer and M. Parsons contributed equally to this article.
Supplemental material for this article may be found at http://ec.asm.org/.

doi:10.1128/EC.05282-11

**TABLE 1** cI V5-tagged proteins and transfectants examined in this study

| Name in Swiss-Prot database (human) | Systematic identifier | Category | Transfectant(s) | Complex observed (kDa) |
|---|---|---|---|---|
| cI$\alpha$ subcomplex | | | | |
| NUAM (NDUFS1) | Tb927.10.12540 | Core | BF SM[a] | No |
| NUBM (NDUFV1) | Tb927.5.450 | Core | BF SM, BF$\Delta$*nukm*, BF *T. evansi* $\Delta$*rel1*, PF 29.13 | 740[b] |
| NUHM (NDUFV2) | Tb927.7.6350 | Core | BF SM, BF NUBM-TAP, BF LIR-HA | 740 |
| NUKM (NDUFS7) | Tb11.47.0017 | Core | BF SM | No |
| NUEM (NDUFA9) | Tb09.244.2620[c] | Conserved accessory | BF SM | No |
| NI8M (NDUFA5) | Tb11.01.8630 | Conserved accessory | BF SM | 740 |
| NB4M (NDUFA6) | Tb927.10.14860 | Conserved accessory | BF SM | 740 |
| ACSL | Tb927.6.2010 | Accessory | BF SM | No |
| cI$\beta$ subcomplex | | | | |
| NI2 M (NDUFB9) | Tb11.01.7460 | Conserved accessory | BF SM, BF NUBM-TAP, BF LIR-HA | 855 |
| LIR | Tb11.01.7090 | Accessory | BF SM, BF$\Delta$*nubm*, BF$\Delta$*nukm*, BF *T. evansi* $\Delta$*rel1*, BF NUBM-TAP, PF 29.13 | 855[b] |

[a] SM, BF single-marker strain.
[b] No complex observed in *T. evansi.*
[c] One of two candidate NUEM genes, the other being Tb927.10.13620 (1).

of a large complex isolated from PFs by immunoprecipitation or tandem affinity purification (TAP) has identified several bona fide cI subunits, including several core proteins (1, 42), although the mitochondrially encoded proteins have not yet been detected. Most recently, RNA interference (RNAi)-mediated knockdown of three core subunits of cI has indicated that this complex is not required for normal growth in cultured PFs but that it may contribute approximately 20% of the total mitochondrial NADH: ubiquinone oxidoreductase activity (61).

Thus far, there have been no reports of intact cI (or cI subcomplexes) in BFs. However, previous findings suggested a potential upregulation in that stage since mRNA levels of several of the mitochondrially encoded cI subunits were shown to be increased compared to the levels in PFs. These include mRNAs that must undergo RNA editing to generate a functional transcript (ND7, ND8, ND9) (31, 49, 57), as well as those that are never edited (ND4, ND5). Indeed, several mitochondrially encoded cI subunit mRNAs are preferentially edited in BFs (31, 56), and the ND7 subunit is fully edited in BFs only (31, 48). Ablation of mitochondrial gene expression is normally lethal in BFs, demonstrating that essential gene products are encoded in the mitochondrial DNA (53). Therefore, we hypothesized that cI could be playing an important role in this stage of the parasite's life cycle. Here we report the presence of cI$\alpha$ and cI$\beta$ subcomplexes in BFs. However, knockout of two core subunits in slender-form BFs revealed that electron transport activity of the complex was irrelevant for *in vitro* or *in vivo* growth of the pathogen. Furthermore, NADH: ubiquinone oxidoreductase activity was not reduced in the knockout mutants. Thus, our findings conclusively demonstrate that the classical function of cI as a proton pump driven by electron transport is insignificant in slender BFs.

## MATERIALS AND METHODS

**Parasites and growth assays.** BF strain 427 *T. b. brucei*, its single-marker derivative (63), and *T. evansi* AnTat 3/3 (55) were grown at 37°C in HMI-9 medium (25) supplemented with 10% heat-inactivated fetal bovine serum (FBS). The *T. evansi* strain employed is a *rel1* null mutant in which the two alleles of the *REL1* locus are occupied by constructs encoding the T7 RNA polymerase and the tetracycline (Tet) repressor, respectively (52). PF strain 29-13, expressing T7 RNA polymerase and Tet repressor, was cultured in SDM-79 medium (JRH Biosciences [7]) with 10% heat-inactivated FBS. Drugs to maintain selection for transgenes were included when relevant: G418 (2.5 $\mu$g/ml for BFs, 15 $\mu$g/ml for PFs), hygromycin (5 $\mu$g/ml for BFs, 50 $\mu$g/ml for PFs), and puromycin (1 $\mu$g/ml for BFs and PFs). PFs and BFs were transfected as described previously (63). Transfected cells were selected in appropriate medium with drugs as described above. Protein expression from Tet-regulated constructs was induced with 1 to 2 $\mu$g/ml of Tet. A list of the cell lines used in this study is provided in Table 1.

For analysis of growth *in vitro* and *in vivo*, wild-type (WT) 427 and knockout lines were maintained in logarithmic phase of growth for 2 days before the start of the experiments (cell number not exceeding $10^6$/ml). For *in vitro* growth assays, $5 \times 10^4$ parasites were inoculated into 1 ml in triplicate. Cell counts were taken every 24 h over a period of 6 days, and cultures were split 1:20 when the number reached $10^6$/ml.

Procedures involving vertebrate animals (rats and mice) followed protocols approved by the institutional IACUC. For *in vivo* assays, BALB/c mice were infected intraperitoneally with $10^4$ cells resuspended in 200 $\mu$l of phosphate-buffered saline (PBS) containing 10 mM glucose (PSG). Parasitemias were scored every 12 to 24 h starting at 72 h postinfection. Blood obtained by tail prick was diluted 200-fold in cell fix solution (3.7% formaldehyde in 1× SSC [1× SSC is 0.15 M NaCl plus 0.015 M sodium citrate]), and parasites were counted microscopically using a Neubauer hemocytometer. Mice were euthanized by $CO_2$ asphyxiation when the parasite number exceeded $10^8$ cells/ml. When needed, large numbers ($1 \times 10^9$ to $3 \times 10^9$) of *T. brucei* BFs were obtained from 1 to 4 infected rats as described previously (28). Rats were provided doxycycline in their drinking water to induce expression of the tagged gene. Briefly, when the parasitemia reached ~$10^8$/ml blood, infected blood was harvested and pooled. The buffy coat containing the trypanosomes was loaded onto a DE52 column, where the red blood cells were retained. The parasites were collected from the flowthrough fraction.

**Plasmids and constructs.** The open reading frames of *NUAM*, *NUHM*, *NUKM*, *NB4M*, *NI2M*, *NI8M*, the LYR4/ISD11-related gene *LIR*, and acyl coenzyme A (CoA)-synthetase/ligase like gene (*ACSL*) were PCR amplified using strain 427 genomic DNA as template and primers that placed HindIII and BamHI restriction enzyme sites and AvrII and XhoI restriction enzyme sites at the 5′ and 3′ ends of the amplicon, respectively (see Table 1 for systematic identifiers and Table S1 in the supplemental material for primers). The products were digested with the corresponding enzymes and were cloned into the *T. brucei* expression vector pT7-3V5-PAC (22), such that three V5 tags were appended to the C terminus of the protein. The *NUBM* PCR product was similarly cloned into pLew79-3V5-

PAC and pT7-MH-TAP vectors. The latter was created in two steps. First, pT7-Myc (gift of David Horn) was modified by deleting the Myc tag and stuffer region and inserting a linker containing AvrII and NsiI sites. We named this intermediate vector pT7-AN. Second, the sequences encoding the Myc, His, and TAP tags of pLew79-MH-TAP were released with AvrII and PstI and cloned in pT7-AN digested with AvrII and NsiI. The vector pT7-3HA-HYG was generated by ligating a linker coding for three repeats of the hemagglutinin (HA) peptide (YPYDVPDYA) plus HindIII, XhoI, and BamHI sites into the AvrII and PstI sites of pT7-AN. The LIR coding region was subcloned from pT7-LIR-V5-PAC into this vector using HindIII and BamHI sites, to yield a C-terminally HA-tagged protein. All relevant regions of the plasmids were confirmed by sequencing. The constructs were linearized by NotI digestion prior to transfection.

To generate BF cell lines lacking cI subunits, approximately 500 bp of the 5′ and 3′ intergenic regions from *NUKM* and *NUBM* was amplified using the primers listed in Table S1 in the supplemental material and cloned into pGEM-T Easy (Promega). Knockout constructs were generated as described previously (38), replacing one allele with the T7 RNA polymerase and *NEO* genes and the other with the Tet repressor and *HYG* genes. After transfection and selection, the resulting BF lines were analyzed by PCR (testing for correct integration of the knockout constructs and absence of the coding sequence) and Southern analysis to identify those that lacked *NUBM* (Δ*nubm*) or *NUKM* (Δ*nukm*).

**Native gel electrophoresis.** To prepare the organellar fraction, $1 \times 10^8$ to $2 \times 10^8$ BF or PF parasites were treated with a final concentration of 0.025% (wt/vol) digitonin in Hank's balanced salt solution (HBSS; Invitrogen) supplemented with protease inhibitors (Roche), as described previously (34, 54). The organellar pellets were solubilized in 100 μl ice-cold HBSS with 1% dodecyl maltoside (DDM) and incubated on ice for 10 min. After centrifugation at 16,000 × *g* for 10 min at 4°C, the supernatant was incubated with 1 U of RNase-free DNase I (Promega) and 10 mM $MgCl_2$ for 10 min on ice. Native gel electrophoresis of the DNase-treated organellar lysates was performed according to published protocols (64, 65), with the following changes. To 80 μl of lysate, we added 10 μl of 1% Ponceau S and 10 μl of 50% glycerol for high-resolution clear native gel electrophoresis (hrCNE) or 5 μl of 5% Coomassie G-250, 5 μl of 1% Ponceau S, and 10 μl of 50% glycerol for blue native gel electrophoresis (BNE). Unless otherwise noted, $10^7$ cell equivalents (approximately 20 μg of protein) for BFs or $5 \times 10^6$ cell equivalents for PFs were loaded onto precast NuPAGE bis-Tris 4 to 16% gradient clear native gels (Invitrogen). For hrCNE, the cathode buffer was supplemented with 0.05% deoxycholate and 0.02% dodecyl maltoside. For BNE, the cathode buffer was supplemented with 0.05% Coomassie G-250, followed by a change to 0.005% Coomassie G-250 after 30 min. Gels were run at 4°C, beginning at 150 V for 1 h and then at 300 V until most of the dye front ran off the gel.

**Immunofluorescence, immunoblot, and immunoprecipitation analysis.** BFs were incubated in prewarmed HMI-9 medium with 60 nM MitoTracker red CMXRos (Invitrogen) at 37°C for 30 min to stain mitochondria. The parasites were then washed, fixed in 3.7% paraformaldehyde (Sigma), and placed on poly-lysine-coated coverslips, before permeabilizing with 0.1% Triton X-100 in PBS. Slides were blocked with a mixture of 5.5% FBS and 10% goat serum. Mouse anti-V5 monoclonal antibody (MAb) was used at 5 μg/ml, followed by fluorescein isothiocyanate-labeled goat anti-mouse IgG2a (Southern Biotech) at 5 μg/ml. Nuclei and kinetoplasts were stained with 4′,6-diamidino-2-phenylindole (DAPI; Sigma). Coverslips were mounted using Prolong antifade reagent (Invitrogen), and samples were viewed with a Delta Vision RT deconvolution microscope with an Olympus UPlan/Apo ×100 1.35-numerical-aperture objective. Images were deconvolved using the conservative ratio option; single deconvolved planes are shown. For Western blots, protein samples ($10^7$ cell equivalents for BFs or $5 \times 10^6$ cell equivalents for PFs) were resolved on precast SDS-polyacrylamide gels (Bio-Rad) and then transferred onto nitrocellulose membranes. Native gels were equilibrated in 1× SDS running buffer for 30 min before transfer onto polyvinylidene difluoride (PVDF) membranes at 20 V overnight at 4°C. Blots were incubated in blocking buffer (Li-Cor Biosciences), followed by either mouse anti-V5 MAb (Invitrogen) at 0.5 μg/ml, mouse anti-dihydrolipoamide dehydrogenase MAb 17 (2, 43) at 1:2,000, or rat anti-HA MAb (Roche) at 1 μg/ml. Secondary goat anti-mouse IgG-IRDye 800CW, goat anti-rat IgG-IRDye 680CW (Li-Cor Biosciences), and goat anti-rabbit IgG-IRDye 680CW (Li-Cor Biosciences) were detected upon scanning on a Li-Cor Odyssey system. In some cases, anti-V5 MAb was directly coupled to IRDye 800CW.

For coimmunoprecipitation analysis, crude organellar fractions were prepared from $10^8$ BFs expressing the proteins of interest as described above and incubated with 100 μl of 30 mg/ml rabbit IgG coupled to magnetic beads, according to the manufacturer's protocol (Invitrogen), with 75 μl of (10 mg/ml) anti-HA MAb 5D8 magnetic beads (MBL) or with anti-HA MAb 1.11 (Covance) and protein G-coupled magnetic beads. After 1 h at 4°C, the beads were washed three times in HBSS supplemented with protease inhibitors and 0.1% DDM (34, 54) and then eluted with SDS-PAGE sample buffer for immunoblot analysis. Aliquots of the initial lysate and nonbound material were reserved for analysis as well.

To obtain proteins for mass spectrometric analysis, solubilized crude organellar fractions were prepared as described above from ~$5 \times 10^9$ BFs harvested from rats. We employed a V5 purification kit, following the manufacturer's protocol (MBL). Briefly, the sample (0.5 ml) was incubated with 40 μl of a 50% slurry of beads bearing anti-V5 MAb 1H6 and washed three times. The bound complexes were eluted with 40 μl of V5 peptide and subjected to native gel electrophoresis. After silver staining, the band at the appropriate molecular mass was excised and provided to the Fred Hutchison Cancer Research Center Proteomics Facility for trypsin digestion and tandem mass spectrometry on an LTQ Deca (experiment 1) or an LTQ OrbiTrap (experiment 2) spectrometer. The resultant spectra were analyzed by X! Tandem (15) and Mascot (45) software, and statistical validation was conducted via Scaffold software (Proteome Software), which utilizes the Bayesian algorithms of Peptide Prophet (30) and Protein Prophet (37) software. High-abundance proteins such as glycosomal and cytoskeletal proteins were eliminated as candidates, and the identified proteins were compared to those previously seen in cI in PFs (1).

**NADH dehydrogenase activity assays.** For in-gel activity assays, hrCNE gels were incubated in 10 ml NADH dehydrogenase assay buffer (2.5 mg/ml nitroblue tetrazolium, 100 μg/ml NADH, and 5 mM Tris HCl, pH 7.4) for ~30 min at 25°C (26). The gel was subsequently stained with Coomassie R-250 to visualize the marker proteins.

For in-solution assays, an organellar preparation containing mitochondria was made as described previously (26). In brief, BF and PF culture pellets containing ~$3 \times 10^8$ cells were lysed hypotonically. The organellar pellets were solubilized in 100 μl 1 M aminocaproic acid with 2% dodecyl maltoside supplemented with protease inhibitors as described above at 4°C for 30 min. The lysates were centrifuged at 16,000 × *g* for 10 min at 4°C. The NADH dehydrogenase assay was carried out in a 500-μl reaction volume containing 10 μl of the clarified lysate in NDH buffer (50 mM potassium phosphate buffer, pH 7.5, 1 mM EDTA, 0.2 mM KCN), 100 μM NADH, and 20 μM coenzyme $Q_2$. The change in absorbance at 340 nm was measured every 10 s for 2 min; reactions were linear for at least 10 min. A unit of activity was defined as the amount of enzyme that catalyzes the oxidation of 1 nmol NADH $min^{-1}$, assuming an extinction coefficient of 6.2 $mm^{-1}$ $cm^{-1}$. Specific activity was expressed in nmol $min^{-1}$ $mg^{-1}$ of protein lysate.

## RESULTS

**Bloodstream forms and procyclic forms possess similarly sized complexes containing putative cI subunits.** Previous proteomic analyses identified canonical and trypanosomatid-specific cI subunits from PF mitochondria (1, 43). To assess whether cI components were present in BFs, monoclonal antibodies 52 and 63, which bind conformational epitopes of unidentified proteins in cI

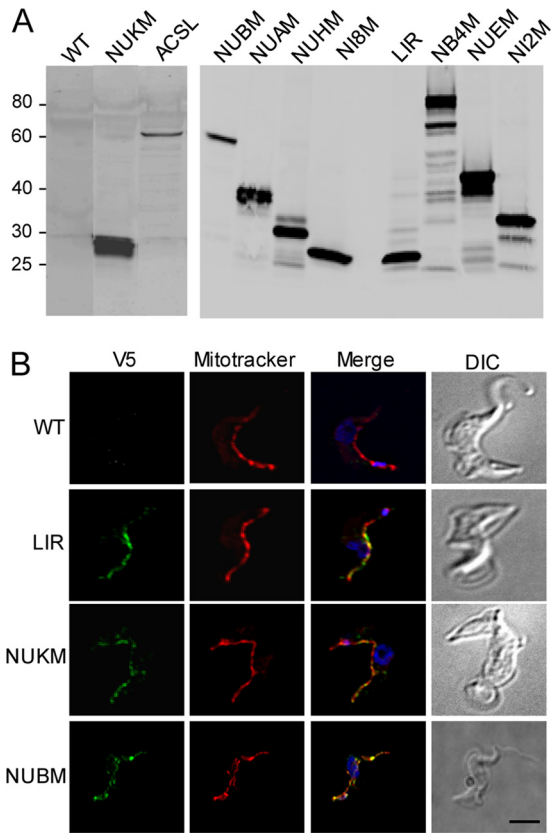


**FIG 1** Tagged putative cI subunits are expressed and localize to the mitochondrion in BFs. (A) Western blot of V5-tagged proteins. Whole-cell lysates of induced (+Tet) and uninduced (−Tet) BFs stably transfected with tagged cI subunits were analyzed by SDS-PAGE (10% gel) and Western blotting using mouse anti-V5 MAb. The predicted molecular masses of the full-length proteins are as follows: NUKM, 23.1 kDa, ACSL, 59.0 kDa; NUBM, 55.3 kDa; NUAM, 33.7 kDa; NUHM, 30.9 kDa; NI8M, 18.8 kDa; LIR, 23.7 kDa, NB4M, 83.4 kDa; NUEM, 42.5 kDa; and NI2M, 36.2 kDa, plus three V5 epitopes (5.4 kDa total). The mass (in kDa) and migration of marker proteins are indicated on this and other figures. Except for NUBM, expression was driven by a T7 promoter which yielded higher expression upon induction with Tet but detectable expression in the absence of Tet. (B) Immunofluorescence analysis. The BF cell transfectants described above were induced with Tet, permeabilized, and stained with mouse anti-V5 MAb (green), MitoTracker (red), and DAPI (blue). In this and other experiments, strain 427 or its single-marker derivative was used as WT BF parasite. DIC, differential interference contrast. Bar = 2 $\mu$m.

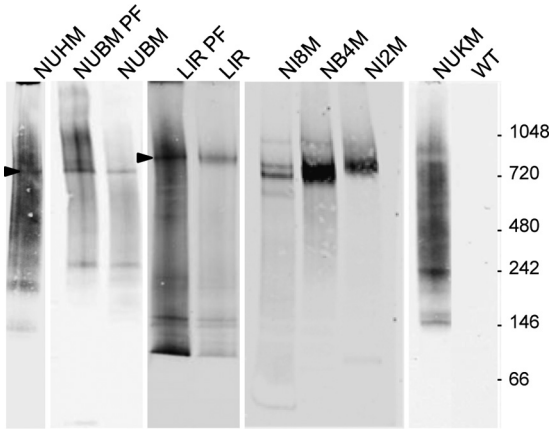


**FIG 2** Native gel analysis of BFs and PFs expressing tagged proteins. Western blotting following hrCNE on 4 to 16% gels. Crude mitochondrial lysates expressing the indicated V5-tagged proteins were separated on native gels, blotted, and probed with mouse anti-V5 MAb. Arrows indicate complexes of interest. Except as noted, samples are from BFs. WT, wild-type BF (strain 427).

subcomplex $\alpha$ (43), were used. These antibodies specifically stained the mitochondrion of BFs (see Fig. S1A in the supplemental material) and detected complexes of similar sizes in BFs and PFs upon glycerol gradient fractionation (Fig. S1B), suggesting the presence of cI-like complexes in BFs.

Native gel electrophoresis provides greater resolution than glycerol gradients and has been successfully used to study bacterial and mitochondrial cI from other systems (64, 65). C-terminally tagged NUBM has been successfully used to study bacterial cI (47). Therefore, to avoid uncertainties using antibodies detecting unidentified conformational determinants (and because attempts to generate useful antisera directed against core subunits were not successful), we combined these techniques to investigate the presence of cI in BF *T. brucei*. Biochemically, cI can be separated into the hydrophobic $\beta$ subcomplex and the $\alpha$ subcomplex, which can be further separated into the hydrophilic $\lambda$ region and the hydrophobic $\gamma$ region (11, 32). We therefore generated BF lines expressing individual V5-tagged versions of core and accessory cI proteins of the $\alpha$ and $\beta$ subcomplexes. These include four core proteins that reside in the hydrophilic part of the cI$\alpha$ subcomplex and participate in electron transfer, namely, NUBM (43), NUKM (alias, NdhK in *T. brucei* [46]), NUAM, and NUHM (see Table 1 for nomenclature and details). We also cloned and expressed V5-tagged versions of three conserved cI$\alpha$ accessory subunits (NB4M, NI8M, and one of two candidate NUEM proteins) and a trypanosomatid-specific accessory protein (an acyl-CoA synthetase/ligase-like protein [ACSL]) previously observed in TAP-tagged pulldowns of cI$\alpha$ subunits in PFs (1, 43). Additionally, NI2M, a conserved cI$\beta$ accessory protein, and an LYR motif protein that was observed in NI2M complexes from PFs were tagged with V5. This LYR motif protein is related to human LYRM4 and *Saccharomyces cerevisiae* ISD11 but, unlike *T. brucei Isd11* (Tb927.10.12000), does not appear to contribute to iron-sulfur cluster biogenesis (44). For simplicity, we will refer to it as LIR (LYR/Isd11 related). Core proteins of the $\beta$ subcomplex are encoded by kinetoplast DNA, precluding their analysis by this approach.

Western blot analysis with anti-V5 antibody confirmed the expression of the tagged proteins in the transfected parasites (Fig. 1A). One major band migrating as predicted from the open reading frame was usually seen when parasites were lysed directly in SDS sample buffer. Each of these proteins was localized to the mitochondrion in BFs by immunofluorescence analysis (Fig. 1B; see Fig. S2 in the supplemental material).

To determine whether the tagged cI proteins exist in complexes, BFs were lysed with digitonin and the organellar fraction containing mitochondria was prepared for native gel analysis by extraction with dodecyl maltoside to gently solubilize cI and other membrane complexes. Following removal of insoluble material, the proteins were separated by hrCNE on 4 to 16% gels and transferred onto PVDF membranes, which were then probed with anti-V5 MAb. As summarized in Table 1 and shown in Fig. 2, major bands averaging 740 kDa were detected in BFs expressing

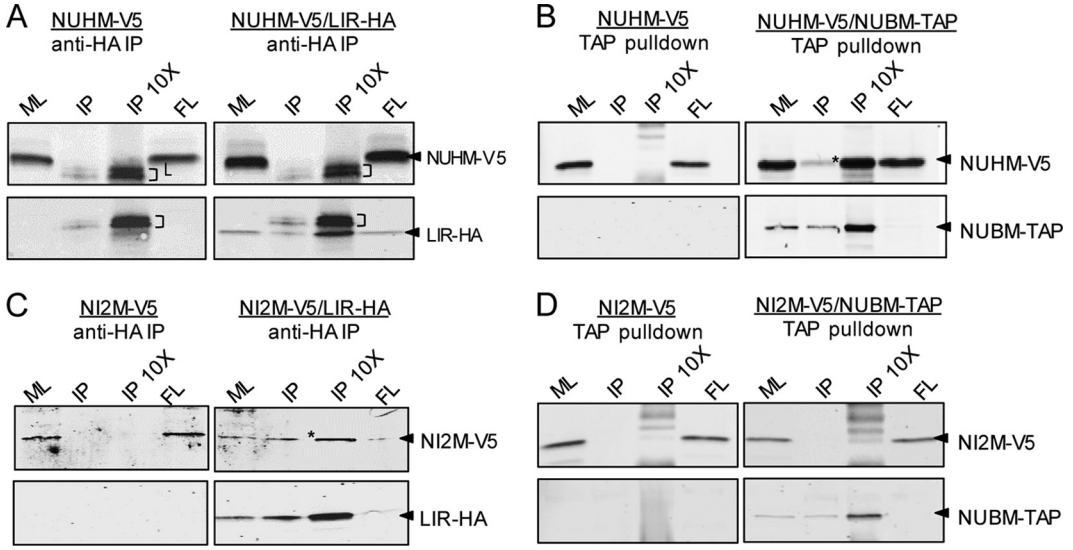


**FIG 3** Coprecipitation analysis. Lysates from BFs expressing NUHM-V5 or NI2M-V5 expressed alone or with NUBM-TAP or LIR-HA were prepared. NUBM-TAP was pulled down by IgG beads (B and D). LIR-HA was pulled down by anti-HA MAb 1.11 and protein G beads (A) or anti-HA MAb 5D8 directly coupled to magnetic beads (C). After electrophoresis on 4 to 12% SDS-polyacrylamide gels, blots were prepared and probed with rabbit anti-goat IgG (to detect TAP tags), rat anti-HA plus IRDye-labeled goat anti-rat IgG, and directly labeled anti-V5 MAb (except for panel A, for which anti-V5 MAb plus labeled goat anti-mouse IgG was employed). ML, crude mitochondrial lysate; FL, flowthrough; IP, pulled-down samples; 10×, 10-fold more cell equivalents were loaded; asterisks; coprecipitation of tagged subunits in panels B and C; brackets in panel A, IgG light chain (L).

the V5-tagged $\alpha$-subcomplex protein NUBM, NUHM, or NB4M, and a similarly sized doublet was seen for NI8M. LIR-V5 and NI2M-V5 complexes averaged 855 kDa (Fig. 2). The size of the complexes did not vary between BFs and PFs, as revealed in parasites expressing NUBM-V5 or LIR-V5 (Fig. 2). Faster-migrating species (seen, for example, for NUBM-V5 and LIR-V5) may represent partially assembled complexes. To confirm that the intact tagged proteins were part of the observed complexes, lanes from selected native gels were subjected to second-dimension SDS-PAGE, followed by Western blot analysis with anti-V5 antibody. At the position of the complex in the first dimension, the second dimension showed tagged proteins at the predicted molecular mass (see Fig. S3 in the supplemental material).

The remaining tagged subunits, NUAM, NUKM, NUEM, and ACSL, all of which are cI$\alpha$ proteins, did not show specific bands that comigrated with the 740-kDa $\alpha$ subcomplex but, rather, migrated as smears with some fainter bands (Fig. 2 shows the example of NUKM; see also Fig. S4 in the supplemental material and the summary in Table 1). NUKM-V5 expressed in PFs also showed a smeared pattern on hrCNE (data not shown). Recent work expressing TAP-tagged NUKM in PFs also failed to detect assembly into a complex (1). These findings suggest poor assembly or retention of these C-terminally tagged proteins or possibly that the tag could be obscured within the complex.

To determine whether the observed complexes contained multiple cI proteins as predicted, we performed coprecipitation analysis on BFs expressing NUHM-V5 alone or along with NUBM-TAP or with LIR-HA (representing the smaller and larger complexes). Similar analyses were performed on parasites expressing NI2M-V5. The lysates were incubated with IgG beads (which capture TAP-tagged proteins) or anti-HA beads. Analysis of the bound material demonstrated that NUHM-V5 was pulled down by IgG beads when NUBM-TAP was expressed, but not in its absence (Fig. 3B). NUHM-V5 did not coprecipitate with LIR-HA (Fig. 3A). Conversely, NI2M was pulled down by anti-HA only in the presence of LIR-HA (Fig. 3C) and was not captured by IgG beads in the presence (or absence) of NUBM-TAP (Fig. 3D). Thus, NUHM and NUBM are in the same complex, presumably cI$\alpha$ (or subassemblies thereof), while LIR and NI2M are associated with a distinct complex, presumably cI$\beta$.

**Multiple cI$\beta$-subcomplex proteins are expressed in BFs.** The composition of the LIR complex in PFs was recently described (1). The similar size of this complex in PFs and BFs (Fig. 2) suggested that their compositions are likely to be similar. To determine whether the proteins observed in the PF LIR complex are also present in the BF LIR complex, we immunoprecipitated LIR-V5 from BFs, eluted the complex from beads with V5 peptide, and subjected the eluate to hrCNE (see Fig. S5 in the supplemental material). The gel piece containing the purified complex was digested with trypsin and subjected to mass spectrometry. Multiple peptides were detected for 11 of 15 proteins known to be associated with the LIR complex in PFs (1) (Table 2). Further sequence analysis suggests that in addition to NI2M, one of these proteins is another conserved cI$\beta$ subunit, NIDM (see Fig. S6 in the supplemental material). Two proteins also proposed to be part of cI (1), although not mapped to a specific subcomplex in that study, were also observed with high confidence. No cI$\alpha$ proteins were detected, other than a single peptide of acyl carrier protein which was previously detected in both subcomplexes (1). While using tagged NUBM to capture the 740-kDa complex from BFs suffered from yields too low to allow similar studies, the native gel analysis, coprecipitation studies, and mass spectrometry together indicate that the 740-kDa and 855-kDa complexes represent the $\alpha$ and $\beta$ subcomplexes of BF cI, respectively.

**Tagged NUBM and LIR do not assemble into complexes in *T. evansi*.** If the complexes that we detected are indeed cI related, then they should be altered in trypanosomes lacking mitochondrially encoded subunits of cI. Therefore, we examined whether

**TABLE 2** LIR complex[a] proteins detected in BFs

| System identifier | Name/GeneDB annotation | Mol wt ($10^3$) | No. of unique peptides | Protein probability (%) |
|---|---|---|---|---|
| Subunits of cI$\beta$ detected (>99% probability) | | | | |
| Tb927.4.4300 | SET domain SF[b] | 63.1 | 10 | >99 |
| Tb927.7.3910 | Nucleoside triphosphate hydrolase SF | 57.6 | 6 | >99 |
| Tb927.8.2530 | Copper chaperone SF | 13.3 | 2 | >99 |
| Tb927.8.5560 | *S*-Adenosylmethionine-dependent methyltransferase SF | 60 | 18 | >99 |
| Tb09.160.4910 | Monooxygenase, putative (FAD/NADP binding domain) | 66.2 | 12 | >99 |
| Tb09.244.2840 | Hypothetical protein, trypanosomatid specific | 23.2 | 13 | >99 |
| Tb927.10.1160 | Hypothetical protein, trypanosomatid specific | 17.5 | 9 | >99 |
| Tb11.01.1690 | NIDM | 30.3 | 5 | >99 |
| Tb11.01.7090 | LIR | 23.7 | 4 | >99 |
| Tb11.01.7460 | NI2M | 36.3 | 6 | >99 |
| Tb11.02.2070[c] | Long-chain fatty acid–CoA ligase protein, putative | 73.4 | 13 | >99 |
| Candidate subunits of cI detected, subcomplex not defined | | | | |
| Tb927.8.6960 | FAD/NADP binding domain SF | 45.4 | 3 | >99 |
| Tb927.10.5500 | Hypothetical protein, trypanosomatid specific | 41.4 | 8 | >99 |
| Subunits of cI$\beta$, presence not confirmed[d] | | | | |
| Tb927.3.860 | Acyl carrier protein | 16.5 | 1 | 98 |
| Tb927.4.440 | Hypothetical protein, trypanosomatid specific | 13.8 | 1 | 58 |
| Tb09.160.0390 | Monooxygenase, putative (FAD/NADP binding domain SF) | 51.4 | 1 | 58 |
| Tb09.211.2780 | Hypothetical protein, trypanosomatid specific | 12.3 | 1 | 58 |

[a] As defined in reference 1.
[b] SF, superfamily.
[c] This protein is distantly related to the $\alpha$-subcomplex protein ACSL.
[d] No mitochondrially encoded candidate subunits were detected in this or previous studies (1, 43).

NUBM and LIR could assemble into complexes in the closely related dyskinetoplastic trypanosome *T. evansi* (strain AnTat 3/3), which has evolved to lack all mitochondrially encoded protein coding genes, including the eight genes predicted to encode core subunits of cI (53) (relocalization to the nuclear genome has been ruled out in AnTat 3/3 [16]). We expressed V5-tagged LIR and NUBM in *T. evansi* and analyzed the samples by immunoblotting. Although the proteins were expressed, as seen by SDS-PAGE and Western blotting, they were not assembled into the complexes seen in *T. brucei* (Fig. 4). The most likely explanation for this observation is that subunits critical for assembly or stability of the cI subcomplexes are missing in *T. evansi* AnTat 3/3. The predicted nuclearly encoded cI subunits are present and, on average, show >99% sequence identity between the *T. brucei* reference genome strain 927 and *T. evansi* strain STIB805 (A. Schnaufer, unpublished data). For example, LIR is identical in amino acid sequence in both, whereas NUBM shows one amino acid change (plus an additional change in the second allele) in *T. evansi*. Thus, these data suggest that both the NUBM complex and the LIR complex require products encoded in the mitochondrial genome for their assembly or stability.

**Electron transfer in cI is not essential in proliferating BFs.** Having established that cI-related complexes are present in *T. brucei* BFs, we next assessed whether cI activity is important in BFs. The flavoprotein NUBM is the first protein to receive electrons from NADH, whereas the iron-sulfur cluster protein NUKM is the last protein in the redox chain and passes electrons to ubiquinone (24). Therefore, to assess whether electron transfer

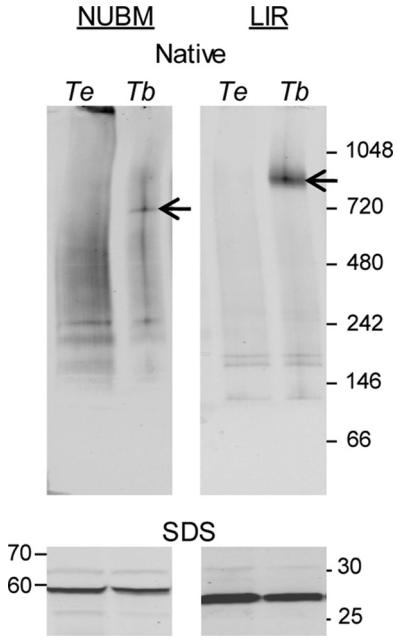


**FIG 4** NUBM-V5 and LIR-V5 complexes are not formed in *T. evansi*. NUBM-V5 and LIR-V5 were expressed in BF *T. brucei* (*Tb*) and *T. evansi* (*Te*) upon Tet induction, and cell equivalents were probed with anti-V5 MAb. (Top) Native gel Western blot, with arrows marking complexes of interest; (bottom) SDS-PAGE Western blot.

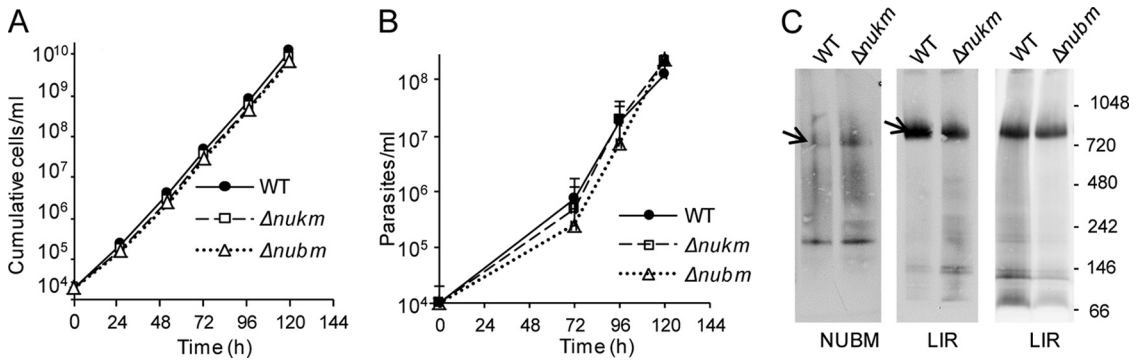


**FIG 5** BFs lacking cI subunits essential for electron transport are viable *in vitro* and *in vivo* and form NUBM and LIR complexes. (A) *In vitro* growth assay. Null mutants Δ*nubm* and Δ*nukm* were compared to the parental wild-type strain for growth *in vitro*. Each point on the lines is the mean of triplicate cultures (the standard deviation was too small to depict). Similar results were obtained in a second experiment. (B) *In vivo* growth assay. Following injection into groups of five mice, the parasitemia was measured daily. Data are represented as mean ± SEM. Similar results were obtained in a second experiment. (C) Native gel Western blot. LIR-V5 was expressed in the Δ*nubm* and Δ*nukm* lines, and NUBM-V5 was expressed in the Δ*nukm* line. The blots were probed with anti-V5. Complexes of interest are indicated by the arrows.

in cI is important to BFs, we generated deletion mutants of these core proteins by homologous recombination (see Fig. S7A in the supplemental material). Generation of the double knockouts Δ*nubm* and Δ*nukm* did not require the presence of a complementing gene. Southern blot analysis showed the absence of the coding sequence and the presence of the expected integration events in Δ*nubm* and Δ*nukm* lines (see Fig. S7B in the supplemental material). The Δ*nubm* and Δ*nukm* BF mutants were compared with wild-type BFs for their ability to grow *in vitro* in standard medium. Cell counts over a period of 7 days indicated no difference in growth rate of the mutants compared to the parental wild-type parasites (Fig. 5A).

We next tested whether the loss of cI electron transfer affected parasite growth *in vivo*. Mice were injected intraperitoneally with wild-type, Δ*nubm*, and Δ*nukm* parasites. Parasitemias were scored until the number reached $10^8$, at which point the animals were euthanized. In all cell lines, parasitemia increased with virtually identical rates (Fig. 5B). These studies demonstrate that the electron transport function of *T. brucei* cI is not essential or even important for growth or virulence in BFs, at least not under these experimental conditions.

The availability of these null mutants allowed us to assess whether the NUBM and LIR complexes required the presence of these core cI subunits for proper assembly. We expressed LIR-V5 in the Δ*nubm* and Δ*nukm* lines and NUBM-V5 in the Δ*nukm* line. There were no discernible differences in the size of the LIR complex in these lines compared to wild type (Fig. 5C), indicating that neither NUBM nor NUKM is required for its assembly. Similarly NUKM appears not to be required for assembly of the NUBM complex, even though the two core proteins typically participate in electron transfer and reside in the hydrophilic λ portion of the α subcomplex of cI. We suggest that the resolution of our gel system is not sufficient to detect the loss of NUKM (23 kDa) from the NUBM complex. Because NUKM-V5 did not assemble into complexes, we were unable to perform the reverse experiment in the Δ*nubm* line.

**In-gel NADH dehydrogenase activity in *T. brucei* is not due to cI.** In-gel catalytic assays are standardly used to detect cI NADH dehydrogenase activity in many systems (9, 65, 66). Such assays have led to reports of cI activity in PF *T. brucei* and in *Phytomonas serpens* (12, 26). Our Δ*nubm* and Δ*nukm* mutant lines provided an opportunity to determine whether the reported activity can be traced to cI in BFs. We also examined dyskinetoplastid mutants *T. brucei* EATRO 164 dk and *T. evansi* AnTat 3/3 as controls, since they lack all mitochondrially encoded subunits of cI. Solubilized crude organellar preparations were separated by hrCNE and stained for NADH dehydrogenase activity using the nitrotetrazolium blue electron acceptor. In PFs and all of the BF samples, including Δ*nubm*, Δ*nukm*, and the dyskinetoplastic strain *T. brucei* EATRO 164 dk, activity was predominantly positioned at ~500 kDa in 4 to 16% hrCNE gels (Fig. 6A), clearly distinct from the position of the cIα complex at 740 kDa on such gels (Fig. 2). Similar results were obtained for *T. evansi* (data not shown). Thus, this activity is not due to cI. The migration of the major NADH dehydrogenase changed with gel conditions. On blue native gels, as used in previous work (26), the major activity band migrated at ~530 kDa (data not shown), while it migrated at ~650 kDa in 3 to 12% hrCNE gels (see Fig. S8 in the supplemental material). On some gels, we observed an additional faint activity band that migrated significantly more slowly than the 1,048-kDa marker in each sample (WT, Δ*nubm*, Δ*nukm*, and PF), indicating that it too is not cI (Fig. S8).

Despite its common use, the nitroblue tetrazolium electron acceptor is not specific for cI. Complexes containing dihydrolipoamide dehydrogenase can also be detected on native gels using NADH and nitroblue tetrazolium as substrates (67). Indeed, immunoblotting of the 4 to 16% native gel with anti-dihydrolipoamide dehydrogenase (Tb11.01.8470) MAb 17 revealed a band at ~500 kDa, the same size as the NADH dehydrogenase activity band (Fig. 6B). As the dihydrolipoamide dehydrogenase subunit is potentially shared between four complexes (glycine cleavage complex, 2-oxoglutarate dehydrogenase, branched-chain α-ketoacid dehydrogenase, and pyruvate dehydrogenase), the observed activity likely results from one of those complexes.

**Complex I does not contribute significantly to NADH: ubiquinone oxidoreductase activity in BFs.** Because the in-gel assay used a general electron acceptor, a specific NADH:ubiquinone oxidoreductase activity assay was performed in wild-type, Δ*nubm*, and Δ*nukm* BF lines using the electron acceptor coen-

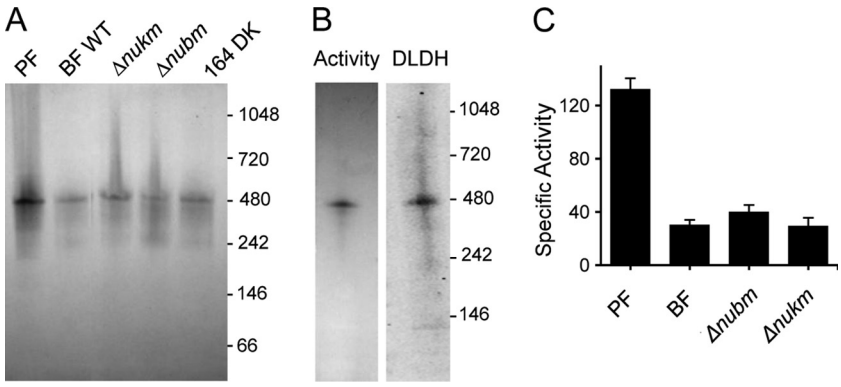


**FIG 6** In-gel NADH dehydrogenase activity is unaltered in NUBM or NUKM deletion mutants and dyskinetoplastic *T. brucei*. (A) In-gel activity assay following hrCNE on 4 to 16% gels. (B) The majority of in-gel NADH dehydrogenase activity comigrates with a dihydrolipoamide dehydrogenase (DLDH)-containing complex. Different lanes from the same gel were analyzed for NADH dehydrogenase activity (left) and by Western blotting using anti-DLDH MAb 17. (C) Complex I does not contribute to specific NADH:ubiquinone oxidoreductase activity in BFs. Lysates from PFs as well as WT, Δ*nubm*, and Δ*nukm* BFs were assayed for NADH:ubiquinone oxidoreductase activity using the specific electron acceptor coenzyme $Q_2$. The specific activities from three independent experiments are expressed as the mean ± SEM in $nmol^{-1}$ $min^{-1}$ mg protein.

zyme $Q_2$. Crude mitochondrial pellets were solubilized in dodecyl maltoside, and the cleared lysates were used for the assay (no activity was observed in the pellet fraction). As a control, we utilized PFs and observed a similar amount of activity compared to that reported by Fang et al. (21), which is about 4-fold higher than that reported by Verner et al. (61). As shown in Fig. 6C, a low level of activity was reproducibly observed in BF lysates, measuring approximately 25% of that seen in PFs at a mean of 30.4 ± 6.2 nmol $min^{-1}$ $mg^{-1}$ protein. In three separate experiments, we observed no reduction in NADH:ubiquinone oxidoreductase activity in the Δ*nubm* or Δ*nukm* mutant line compared to the wild-type parental line (Fig. 6C), with an average of 34.4 ± 8.6 and 29.7 ± 10.2 nmol $min^{-1}$ $mg^{-1}$ protein, respectively. Considering the critical role of NUBM and NUKM proteins in cI-mediated transfer of electrons from NADH to ubiquinone, the data demonstrate that little if any cI activity is present in BFs and indicate that the low level of NADH:ubiquinone oxidoreductase activity observed in this assay is due to other enzymes.

## DISCUSSION

On the basis of low levels of NADH:ubiquinone oxidoreductase activity and its low sensitivity to the cI inhibitor rotenone, the presence and functionality of cI in *T. brucei* have been debated (40). Comparative genomics recognized the homologues of 12 core and 7 conserved accessory cI subunits in the nuclear and mitochondrial genomes of *T. brucei* (29, 40), and in PFs, 4 cI core subunits and the 7 conserved accessory subunits have been identified by proteomic analysis (1, 29, 43). Recent work suggests that cI contributes about 20% of the NADH dehydrogenase activity in PFs, even though it appears not to be essential (61). Since there is evidence that several mitochondrially encoded cI subunit mRNAs are fully edited preferentially or even exclusively in BFs (31, 48, 56), we tested the hypothesis that cI has an important role in this stage of the parasite's life cycle. In this report, we provide the first evidence that the two cI subcomplexes, α and β, are present in the pathogenic BF stage. However, null mutants for key catalytic subunits showed normal growth under *in vitro* and *in vivo* conditions, raising the question of why *T. brucei* invests considerable energy into the biogenesis of this largest complex of the respiratory chain.

The α subcomplexes from BFs and PFs comigrated on hrCNE, as did the β subcomplexes, suggesting that their subunit compositions are quite similar in both stages. Indeed, mass spectrometric analysis of LIR-V5 pulldowns from BFs contained multiple proteins observed in similar pulldowns from PFs (Table 2; see also reference 1). While a few accessory proteins detected in PF cIβ remain unconfirmed to be part of BF cIβ, this might reflect the limited amounts of protein available for analysis rather than a true difference. It is interesting that there are no data as yet that strongly support the association of the two subcomplexes in either stage. The two most extreme explanations for the lack of evidence for physical association are that (i) the subcomplexes are associated *in vivo* but the structure is disturbed by the experimental conditions or (ii) the LIR complex is distinct from cI. In defense of the first proposal, the physical separation of cI into subcomplexes is well-known (11, 32). Although the conditions that we used are similar to those employed to study cI from other species, the complete *T. brucei* cI complex might be more susceptible to dissociation than is typical or undergo only limited assembly into the complete complex *in vivo*. With respect to the second proposal, the proteins that coprecipitated with tagged LIR here and in PFs (1) included only two proteins that are identifiable members of cIβ, NI2M and NIDM. Two proteins important for the proton-pumping activity of cI are not identifiable via bioinformatic analysis, raising the intriguing possibility that the LIR complex represents a diverged version of the hydrophobic arm of cI that has adopted additional subunits and functions.

Our data suggest that mitochondrially encoded proteins are required for the assembly or maintenance of the NUBM-V5- and LIR-V5-containing complexes. *T. brucei* NUBM-V5 and LIR-V5, when expressed in *T. evansi*, which lacks mitochondrially encoded proteins, did not assemble in large complexes. It is unlikely that this finding reflects sequence divergence between *T. brucei* and *T. evansi* since their LIR and NUBM protein sequences show 100% and >99% identities, respectively. *T. brucei* mitochondrial DNA is predicted to encode at least eight core cI subunits, including ND8 (NUIM) and ND9 (NUGM), components of the hydrophilic arm, thus explaining why the NUBM complex does not properly form in *T. evansi*. Obvious candidates for mitochondrially en-

coded proteins essential for the LIR complex are the mitochondrially encoded ND4 and ND5 subunits of cI$\beta$ and the four unidentified reading frames.

The NUBM and the NUKM proteins are essential for cI electron transport activity (8, 19, 33). The two cI subunit-knockout strains, Δ*nubm* and Δ*nukm*, were indistinguishable from wild type with respect to growth *in vitro* and virulence *in vivo*. The latter finding argues that the lack of a requirement for cI is not simply the result of long-term culture in replete medium. In addition, comparison of NADH:ubiquinone oxidoreductase activity in crude mitochondrial fractions showed no significant differences between wild type, Δ*nubm*, and Δ*nukm* parasites (Fig. 6). Similarly, none of the bands showing NADH dehydrogenase activity in the in-gel assay corresponded with the cI$\alpha$ complex. Thus, electron transport activity of cI is not essential or even detectable in slender BFs. These data indicate that cI is not catalytically active in this developmental stage or is present in very low abundance.

Although there is now evidence for the presence of cI-like subcomplexes in two life-cycle stages of *T. brucei*, cI functions in the parasite remain enigmatic. In *Plasmodium* and *Saccharomyces cerevisiae*, the absence of cI function reflects the loss of all cI core genes, a situation dramatically different from that in trypanosomes. Our comparison of nucleotide substitution rates in genes encoding bona fide cI subunits of *T. b. brucei* and *T. congolense* (using the Nei-Gojobori model [36] in the MEGA5 software [58]) shows that the ratio of synonymous and nonsynonymous changes is similar to that of known essential genes (see Table S2 in the supplemental material). These findings indicate that purifying selection is acting to maintain the functionality of these genes in African trypanosomes, pointing to an important role at some point in the parasite life cycle. Given that the NADH:ubiquinone oxidoreductase activity of cI is irrelevant in slender BFs and PFs, when might cI be important? The strain that we used does not develop into transitional stumpy BFs, but Bienen and coworkers proposed a critical role for cI in generating the mitochondrial membrane potential and possibly ATP synthesis in that stage (4). In a high-throughput RNAi study (3), about 30% of the cI$\alpha$ and cI$\beta$ proteins appeared to be important either in BFs in the process of differentiating to PFs or under all conditions (slender BFs, differentiating BFs, and PFs). Interestingly, five subunits were identified only in the differentiation experiment. However, none of the hits under any condition were core subunits, and the majority were trypanosomatid specific. Of course, cI function could be important in other insect stages, such as epimastigotes and metacyclic forms, which remain relatively inaccessible and understudied. Nonetheless, the evolutionary conservation of the identified bona fide subunits of cI in among trypanosomatids such as *T. brucei*, *T. congolense*, *T. cruzi*, or *Leishmania* spp. indicates that certain, but possibly varying, functions of cI may have been retained across the trypanosomatid order. Interestingly, *L. tarentolae* was reported to lose minicircles required for editing of mitochondrially encoded cI mRNAs after prolonged culture of the promastigote stage (59), supporting the notion of a stage-specific role. In contrast, mitochondrial DNA deletions affecting cI subunits in *T. cruzi* lineages were taken as evidence that the complex does not have an important role in that organism (10). A potential role of cI that is not directly related to its classical enzymatic function in electron transfer and proton translocation is its association with certain accessory factors. For example, acyl carrier protein has been found to be associated with cI in PF *T. brucei* (43) and some other organisms (23), and this protein is essential in BF *T. brucei* (13). However, the viability and virulence of dyskinetoplastic *T. evansi* parasites, which do not appear to assemble these complexes, suggest that any such functions do not require assembly of those subunits into the full complex or that such a requirement has been circumvented in these parasites.

Although we did not find evidence for any contribution of cI to NADH:ubiquinone oxidoreductase activity in BF *T. brucei*, this activity is clearly present, albeit at reduced levels compared to PF cells (Fig. 6C). The alternative NADH dehydrogenase (NDH2) activity is capable of using the same electron acceptor and may thus be the major cause of this activity in BF (20, 61). Studies are under way in our laboratories to test the importance of NDH2 to wild-type and cI-deficient mutant *T. brucei* parasites. Coincidentally, our work helps to explain why BF *T. brucei* may have a requirement for a mitochondrial NADH dehydrogenase activity in the first place. The in-gel activity assay showed a prominent 500-kDa band in lysates from PF, BF wild-type, Δ*nubm*, and Δ*nukm* samples (Fig. 6A). While this activity was previously interpreted to be that of *T. brucei* cI (26), our data suggest that it can be ascribed to a complex containing dihydrolipoamide dehydrogenase (Fig. 6B). A good candidate is the glycine cleavage complex, an activity likely essential for 1-carbon metabolism in *T. brucei* (35, 51). Mitochondrial NADH dehydrogenase activity would therefore be required to regenerate NAD consumed by dihydrolipoamide dehydrogenase.

## ACKNOWLEDGMENTS

We thank Bryan Jensen for many helpful discussions, Yuko Ogata for mass spectrometry, Peter Askovich for assistance in analysis of proteomic data, Darren Obbard for help with the evolutionary analysis, and the Wellcome Trust Sanger Institute for making the *T. congolense* IL-3000 sequences available through the GeneDB and TryTrypDB websites prior to publication. We also thank our intern Jimena Diaz for assistance with immunofluorescence assays.

Jimena Diaz was supported by grant 5R25DK07835-05 from the National Institute of Diabetes and Digestive and Kidney Diseases. This work was supported by grant R01AI69057 to M.P. and A.S. from the National Institute of Allergy and Infectious Diseases and grant RA0568 from the United Kingdom Medical Research Council to A.S.

We are solely responsible for the contents.

## REFERENCES

1. **Acestor N, et al.** 2011. *Trypanosoma brucei* mitochondrial respiratome: composition and organization in procyclic form. Mol. Cell. Proteomics **10**:M110.006908.
2. **Allen TE, et al.** 1998. Association of guide RNA binding protein gBP21 with active RNA editing complexes in *Trypanosoma brucei*. Mol. Cell. Biol. **18**:6014–6022.
3. **Alsford S, et al.** 2011. High throughput phenotyping using parallel sequencing of RNA interference targets in the African trypanosome. Genome Res. **21**:915–924.
4. **Bienen EJ, Saric M, Pollakis G, Grady RW, Clarkson AB Jr.** 1991. Mitochondrial development in *Trypanosoma brucei brucei* transitional bloodstream forms. Mol. Biochem. Parasitol. **45**:185–192.
5. **Brown BS, Chi TB, Williams N.** 2001. The *Trypanosoma brucei* mitochondrial ATP synthase is developmentally regulated at the level of transcript stability. Mol. Biochem. Parasitol. **115**:177–187.
6. **Brown SV, Hosking P, Li J, Williams N.** 2006. ATP synthase is responsible for maintaining mitochondrial membrane potential in bloodstream form *Trypanosoma brucei.* Eukaryot. Cell **5**:45–53.
7. **Brun R, Schoenonberger M.** 1979. Cultivation and in vitro cloning of procyclic culture forms of *Trypanosoma brucei* in a semi-defined medium. Acta Trop. **36**:289–292.

8. **Bych K, et al.** 2008. The iron-sulphur protein Ind1 is required for effective complex I assembly. EMBO J. **27**:1736–1746.
9. **Cardol P, Matagne RF, Remacle C.** 2002. Impact of mutations affecting ND mitochondria-encoded subunits on the activity and assembly of complex I in *Chlamydomonas.* Implication for the structural organization of the enzyme. J. Mol. Biol. **319**:1211–1221.
10. **Carranza JC, et al.** 2009. *Trypanosoma cruzi* maxicircle heterogeneity in Chagas disease patients from Brazil. Int. J. Parasitol. **39**:963–973.
11. **Carroll J, Fearnley IM, Shannon RJ, Hirst J, Walker JE.** 2003. Analysis of the subunit composition of complex I from bovine heart mitochondria. Mol. Cell. Proteomics **2**:117–126.
12. **Cermakova P, Verner Z, Man P, Lukes J, Horvath A.** 2007. Characterization of the NADH:ubiquinone oxidoreductase (complex I) in the trypanosomatid *Phytomonas serpens* (Kinetoplastida). FEBS J. **274**:3150–3158.
13. **Clayton AM, et al.** 2011. Depletion of mitochondrial acyl carrier protein in bloodstream-form Trypanosoma brucei causes a kinetoplast segregation defect. Eukaryot. Cell **10**:286–292.
14. **Coustou V, et al.** 2008. Glucose-induced remodelling of intermediary and energy metabolism in procyclic *Trypanosoma brucei.* J. Biol. Chem. **283**:16342–16354.
15. **Craig R, Beavis RC.** 2004. TANDEM: matching proteins with tandem mass spectra. Bioinformatics **20**:1466–1467.
16. **Domingo GJ, et al.** 2003. Dyskinetoplastic *Trypanosoma brucei* contains functional editing complexes. Eukaryot. Cell **2**:569–577.
17. **Drose S, et al.** 2011. Functional dissection of the proton pumping modules of mitochondrial complex I. PLoS Biol. **9**:e1001128.
18. **Efremov RG, Baradaran R, Sazanov LA.** 2010. The architecture of respiratory complex I. Nature **465**:441–445.
19. **Falk MJ, et al.** 2009. Subcomplex Ilambda specifically controls integrated mitochondrial functions in Caenorhabditis elegans. PLoS One **4**:e6607.
20. **Fang J, Beattie DS.** 2003. Identification of a gene encoding a 54 kDa alternative NADH dehydrogenase in *Trypanosoma brucei.* Mol. Biochem. Parasitol. **127**:73–77.
21. **Fang J, Wang Y, Beattie DS.** 2001. Isolation and characterization of complex I, rotenone-sensitive NADH: ubiquinone oxidoreductase, from the procyclic forms of *Trypanosoma brucei.* Eur. J. Biochem. **268**:3075–3082.
22. **Flaspohler JA, Jensen BC, Saveria T, Kifer CT, Parsons M.** 2010. A novel protein kinase localized to lipid droplets is required for droplet biogenesis in trypanosomes. Eukaryot. Cell **9**:1702–1710.
23. **Gabaldon T, Rainey D, Huynen MA.** 2005. Tracing the evolution of a large protein complex in the eukaryotes, NADH:ubiquinone oxidoreductase (complex I). J. Mol. Biol. **348**:857–870.
24. **Hirst J.** 2010. Towards the molecular mechanism of respiratory complex I. Biochem. J. **425**:327–339.
25. **Hirumi H, Hirumi K.** 1989. Continuous cultivation of *Trypanosoma brucei* blood stream forms in a medium containing a low concentration of serum protein without feeder cells. J. Parasitol. **75**:985–989.
26. **Horvath A, et al.** 2005. Downregulation of the nuclear-encoded subunits of the complexes III and IV disrupts their respective complexes but not complex I in procyclic *Trypanosoma brucei.* Mol. Microbiol. **58**:116–130.
27. **Hunte C, Zickermann V, Brandt U.** 2010. Functional modules and structural basis of conformational coupling in mitochondrial complex I. Science **329**:448–451.
28. **Jensen BC, Sivam D, Kifer CT, Myler PJ, Parsons M.** 2009. Widespread variation in transcript abundance within and across developmental stages of *Trypanosoma brucei.* BMC Genomics **10**:482.
29. **Kannan S, Burger G.** 2008. Unassigned MURF1 of kinetoplastids codes for NADH dehydrogenase subunit 2. BMC Genomics **9**:455.
30. **Keller A, Nesvizhskii AI, Kolker E, Aebersold R.** 2002. Empirical statistical model to estimate the accuracy of peptide identifications made by MS/MS and database search. Anal. Chem. **74**:5383–5392.
31. **Koslowsky DJ, Bhat GJ, Perrollaz AL, Feagin JE, Stuart K.** 1990. The *MURF3* gene of *Trypanosoma brucei* contains multiple domains of extensive editing and is homologous to a subunit of NADH dehydrogenase. Cell **62**:901–911.
32. **Lazarou M, Thorburn DR, Ryan MT, McKenzie M.** 2009. Assembly of mitochondrial complex I and defects in disease. Biochim. Biophys. Acta **1793**:78–88.
33. **Lebon S, et al.** 2007. A novel mutation of the NDUFS7 gene leads to activation of a cryptic exon and impaired assembly of mitochondrial complex I in a patient with Leigh syndrome. Mol. Genet. Metab. **92**:104–108.
34. **Moyersoen J, et al.** 2003. Characterization of *Trypanosoma brucei* PEX14 and its role in the import of glycosomal matrix proteins. Eur. J. Biochem. **270**:2059–2067.
35. **Muller M, Papadopoulou B.** 2010. Stage-specific expression of the glycine cleavage complex subunits in *Leishmania infantum.* Mol. Biochem. Parasitol. **170**:17–27.
36. **Nei M, Gojobori T.** 1986. Simple methods for estimating the numbers of synonymous and nonsynonymous nucleotide substitutions. Mol. Biol. Evol. **3**:418–426.
37. **Nesvizhskii AI, Keller A, Kolker E, Aebersold R.** 2003. A statistical model for identifying proteins by tandem mass spectrometry. Anal. Chem. **75**:4646–4658.
38. **Ochatt CM, et al.** 1999. Conditional expression of glycosylphosphatidylinositol phospholipase C in *Trypanosoma brucei.* Mol. Biochem. Parasitol. **103**:35–48.
39. **Opperdoes FR.** 1987. Compartmentation of carbohydrate metabolism in trypanosomes. Annu. Rev. Microbiol. **41**:127–151.
40. **Opperdoes FR, Michels PA.** 2008. Complex I of Trypanosomatidae: does it exist? Trends Parasitol. **24**:310–317.
41. **Pagliarini DJ, et al.** 2008. A mitochondrial protein compendium elucidates complex I disease biology. Cell **134**:112–123.
42. **Panigrahi AK, et al.** 2009. A comprehensive analysis of *Trypanosoma brucei* mitochondrial proteome. Proteomics **9**:434–450.
43. **Panigrahi AK, et al.** 2008. Mitochondrial complexes in *Trypanosoma brucei*: a novel complex and a unique oxidoreductase complex. Mol. Cell. Proteomics **7**:534–545.
44. **Paris Z, et al.** 2010. The Fe/S cluster assembly protein Isd11 is essential for tRNA thiolation in Trypanosoma brucei. J. Biol. Chem. **285**:22394–22402.
45. **Perkins DN, Pappin DJ, Creasy DM, Cottrell JS.** 1999. Probability-based protein identification by searching sequence databases using mass spectrometry data. Electrophoresis **20**:3551–3567.
46. **Peterson GC, Souza AE, Parsons M.** 1993. Characterization of a *Trypanosoma brucei* nuclear gene encoding a protein homologous to a subunit of bovine NADH:ubiquinone oxidoreductase (complex I). Mol. Biochem. Parasitol. **58**:63–70.
47. **Pohl T, Uhlmann M, Kaufenstein M, Friedrich T.** 2007. Lambda Red-mediated mutagenesis and efficient large scale affinity purification of the Escherichia coli NADH:ubiquinone oxidoreductase (complex I). Biochemistry **46**:10694–10702.
48. **Read LK, Stankey KA, Fish WR, Muthiani AM, Stuart K.** 1994. Developmental regulation of RNA editing and polyadenylation in four life cycle stages of *Trypanosoma congolense.* Mol. Biochem. Parasitol. **68**:297–306.
49. **Read LK, Wilson KD, Myler PJ, Stuart K.** 1994. Editing of *Trypanosoma brucei* maxicircle CR5 mRNA generates variable carboxy terminal predicted protein sequences. Nucleic Acids Res. **22**:1489–1495.
50. **Remacle C, Barbieri MR, Cardol P, Hamel PP.** 2008. Eukaryotic complex I: functional diversity and experimental systems to unravel the assembly process. Mol. Genet. Genomics **280**:93–110.
51. **Roldan A, Comini MA, Crispo M, Krauth-Siegel RL.** 2011. Lipoamide dehydrogenase is essential for both bloodstream and procyclic *Trypanosoma brucei.* Mol. Microbiol. **81**:623–639.
52. **Schnaufer A, Clark-Walker GD, Steinberg AG, Stuart K.** 2005. The F1-ATP synthase complex in bloodstream stage trypanosomes has an unusual and essential function. EMBO J. **24**:4029–4040.
53. **Schnaufer A, Domingo GJ, Stuart K.** 2002. Natural and induced dyskinetoplastic trypanosomatids: how to live without mitochondrial DNA. Int. J. Parasitol. **32**:1071–1084.
54. **Smid O, et al.** 2006. Knock-downs of iron-sulfur cluster assembly proteins IscS and IscU down-regulate the active mitochondrion of procyclic *Trypanosoma brucei.* J. Biol. Chem. **281**:28679–28686.
55. **Songa EB, et al.** 1990. Evidence for kinetoplast and nuclear DNA homogeneity in *Trypanosoma evansi* isolates. Mol. Biochem. Parasitol. **43**:167–179.
56. **Souza AE, Myler PJ, Stuart K.** 1992. Maxicircle CR1 transcripts of *Trypanosoma brucei* are edited and developmentally regulated and encode a putative iron-sulfur protein homologous to an NADH dehydrogenase subunit. Mol. Cell. Biol. **12**:2100–2107.
57. **Souza AE, Shu HH, Read LK, Myler PJ, Stuart KD.** 1993. Extensive editing of CR2 maxicircle transcripts of *Trypanosoma brucei* predicts a protein with homology to a subunit of NADH dehydrogenase. Mol. Cell. Biol. **13**:6832–6840.
58. **Tamura K, et al.** 2011. MEGA5: molecular evolutionary genetics analysis using maximum likelihood, evolutionary distance, and maximum parsimony methods. Mol. Biol. Evol. **28**:2731–2739.

59. **Thiemann OH, Maslov DA, Simpson L.** 1994. Disruption of RNA editing in *Leishmania tarentolae* by the loss of minicircle-encoded guide RNA genes. EMBO J. **13**:5689–5700.
60. **Tielens AG, Van Hellemond JJ.** 2009. Surprising variety in energy metabolism within Trypanosomatidae. Trends Parasitol. **10**:482–490.
61. **Verner Z, et al.** 2010. Complex I (NADH:ubiquinone oxidoreductase) is active in but non-essential for procyclic *Trypanosoma brucei*. Mol. Biochem. Parasitol. **175**:196–200.
62. **Vickerman K.** 1965. Polymorphism and mitochondrial activity in sleeping sickness trypanosomes. Nature **208**:762–766.
63. **Wirtz E, Leal S, Ochatt C, Cross GA.** 1999. A tightly regulated inducible expression system for conditional gene knock-outs and dominant-negative genetics in *Trypanosoma brucei*. Mol. Biochem. Parasitol. **99**:89–101.
64. **Wittig I, Braun HP, Schagger H.** 2006. Blue native PAGE. Nat. Protoc. **1**:418–428.
65. **Wittig I, Schagger H.** 2008. Features and applications of blue-native and clear-native electrophoresis. Proteomics **8**:3974–3990.
66. **Yan LJ, Forster MJ.** 2009. Resolving mitochondrial protein complexes using nongradient blue native polyacrylamide gel electrophoresis. Anal. Biochem. **389**:143–149.
67. **Yan LJ, Yang SH, Shu H, Prokai L, Forster MJ.** 2007. Histochemical staining and quantification of dihydrolipoamide dehydrogenase diaphorase activity using blue native PAGE. Electrophoresis **28**:1036–1045.
68. **Zickermann V, et al.** 2009. Architecture of complex I and its implications for electron transfer and proton pumping. Biochim. Biophys. Acta **1787**: 574–583.